CARBON 49 (2011) 1561–1567

available at www.sciencedirect.com

ScienceDirect

journal homepage: www.elsevier.com/locate/carbon

A first-principles study of calcium-decorated, boron-doped graphene for high capacity hydrogen storage

Elham Beheshti, Alireza Nojeh, Peyman Servati *

Electrical and Computer Engineering, University of British Columbia, Vancouver, British Columbia, Canada V6T 1Z4

ARTICLE INFO

Article history:
Received 30 June 2010
Accepted 10 December 2010
Available online 21 December 2010

ABSTRACT

Hydrogen adsorption and storage on calcium-decorated, boron-doped graphene was explored using density functional theory simulations based on local density approximation and generalized gradient approximation methods. The clustering problem for calcium-decorated graphene was investigated and it was shown that individual calcium atoms are not stable on pure graphene, and formation of aggregates is favorable. Substitutional boron doping can eliminate the clustering problem for Ca atoms on graphene. Up to four hydrogen molecules can stably bind to a Ca atom on a graphene plane with substitutional doping of a single boron atom. The average binding energy of ~0.4 eV/H_2 is in the range that permits H_2 recycling at ambient conditions. Two binding mechanisms contribute to the adsorption of H_2 molecules: polarization of the H_2 molecule under the electric field produced by the Ca–graphene dipole, and hybridization of the 3*d* orbitals of Ca with the σ orbitals of H_2. Double-sided Ca-decorated graphene doped with individual boron atoms of 12 at.% can theoretically reach a gravimetric capacity of 8.38 wt.% hydrogen.

1. Introduction

Hydrogen has been viewed as a clean energy carrier that could replace fossil fuels, particularly for transportation applications including hydrogen fuel cell vehicles [1]. One of the main challenges in developing this technology is a compact, safe and affordable storage system. A desirable system is capable of storing hydrogen with high gravimetric and volumetric densities at near room temperature and ambient pressure. The US Department of Energy has set a system target of 9 wt.% by 2015. Furthermore, hydrogen recycling (hydrogen adsorption and desorption) should be performed reversibly in a feasible range of temperature and pressure, which requires the optimal hydrogen adsorption energy of 0.2–0.4 eV/H_2 [2,3]. This range of energy is intermediate between the physisorbed and chemisorbed states. Many different techniques such as using metal hydrides, liquefied hydrogen or high pressure tanks have been investigated for hydrogen storage; nevertheless, these techniques have several drawbacks such as low capacity, non-reversibility or safety problems. Recently, carbon nanomaterials with high specific surface area have been widely studied for hydrogen storage [4–6]. However, for carbon in any form, the interaction with H_2 is through weak van der Waals forces [7–9] with low binding energies for storage at ambient conditions.

In recent years, many studies have been devoted to functionalizing the surface of carbon nanostructures with transition metals (TMs) [10–13] to improve binding energy. A TM atom interacts with the carbon substrate and hydrogen molecules through Dewar [14] and Kubas [15] interactions, respectively. The combination of these interactions, in which the TM's 3*d* orbitals are involved, enhances the binding energy. Yildirim et al. [11] and Zhao et al. [12] reported that TM-coated fullerenes and nanotubes can store up to 8 wt.% hydrogen with an average binding energy of 0.3 eV/H_2. For estimation of capacity, TM atoms were assumed to be uniformly distributed on the surface. However, because of high cohesive energy, TM atoms tend to cluster on the surface

* *Corresponding author:* Fax: +1 604 822 5949.
E-mail address: peymans@ece.ubc.ca (P. Servati).
0008-6223/$ - see front matter
doi:10.1016/j.carbon.2010.12.023

of carbon nanostructures and it is difficult to achieve uniformly-coated monolayers of TM atoms experimentally. Consequently, the achievable hydrogen storage capacity is low [10,16,17]. Moreover, TM-coated systems are highly reactive, leading to a dissociative adsorption of the first hydrogen molecule [12].

Metals with smaller cohesive energy such as alkali metals (AM) [18,19] or alkaline earth metals (AEM) can be used to decrease clustering. Although alkali atoms can be coated uniformly, the binding sites for these systems are too weak and the nature of the bonding remains physisorption [20]. Calcium, the first AEM atom with empty 3*d* orbitals, has recently emerged as the preferred material for improving the storage capacity in carbon nanostructures [21–24]. Yoon et al. [21] have suggested Ca-coated C_{60} fullerenes ($Ca_{32}C_{60}$) can store 2.7 H_2 per Ca, resulting in a theoretical 8.4 wt.% capacity. Using density functional theory (DFT), they have shown that among AEM atoms, Be and Mg cannot be stabilized on C_{60} whereas Ca can decorate these materials through electron donation/back-donation mechanisms, involving Ca's empty 3*d* orbitals [21]. This mechanism stabilizes the chemical interaction between Ca and the carbon atoms. Moreover, Ca binds with hydrogen more strongly than AM atoms or other AEM atoms (i.e. Be and Mg) due to the hybridization of its 3*d* orbitals with hydrogen's σ orbitals. Despite all these advantages and lower cohesive energy (~1.8 eV) of Ca [25], aggregation of Ca atoms takes place on graphitic materials as Ca's binding energy on the carbon absorbent is still lower than that of Ca bulk structure [23,26].

In this paper, we investigate the adsorption of hydrogen on calcium-decorated boron-doped graphene using first-principles calculations. Graphene, a monolayer of graphite, can be a precursor to C_{60} and carbon nanotubes and demonstrates unusual electronic and magnetic properties [27]. Considering both sides of the monolayer, graphene has a high specific surface area (2630 $m^2 g^{-1}$), higher than the outer surface area of nanotubes [28]. Here, we show that individually dispersed Ca atoms that bond to both sides of a graphene plane can each take 4 hydrogen molecules, which results in a storage capacity of 8.32 wt.% for a dense coverage of one Ca atom on each (2×2) cell. To achieve a dense coverage of Ca atoms without aggregation, the adsorption energy of individual Ca atoms on graphene must be enhanced. Yang et al. [25] have demonstrated that the stability of individual Ca atoms on graphene can be significantly improved with the presence of pentagonal or octagonal defects. Here, we explore boron substitutional doping as a solution for the clustering problem of Ca atoms. The empty p_z orbital of boron acts as a strong charge acceptor and consequently enhances the adsorption energy of Ca on graphene. Boron can be easily incorporated substitutionally in the hexagonal structure of graphene and boron-doped graphene has been synthesized experimentally [29,30].

2. Simulation details

Our calculations were performed using DFT and the SIESTA software package [31]. The self-consistent DFT code is based on a numerical atomic basis set and the core electrons are replaced by norm-conserving pseudopotentials in their fully nonlocal form [32]. The pseudopotentials were constructed using the Troullier and Martins parametrization [33] to describe the ion–electron interactions. The exchange and correlation potential was treated using the local density approximation (LDA) with Perdew–Zunger parametrization [34]. Furthermore, we compared the LDA results with those of the generalized gradient approximation (GGA) with the Perdew–Burke–Ernzerhof (PBE) functional [35]. The use of these approximations with DFT calculations to describe van der Waals contributions is still controversial. Previous studies have shown that GGA underestimates the relatively weak binding energies, whereas LDA overestimates them [36,37]. To evaluate the reliability of our LDA and GGA calculations, we have also performed second-order Moller–Plesset (MP2) perturbation theory calculations [38] that may improve accuracy for weak van der Waals contributions as will be explained later. We observed that LDA yields energy and structure values close to those calculated by MP2.

The pseudopotential for Ca is constructed using a partial core correction [39], which accounts for the nonlinear interaction of the core and valence densities. A double-ζ singly polarized (DZP) basis set was selected, and atomic orbitals with a fixed common energy shift of 50 meV for all atomic species was used to obtain a well balanced basis. A diffuse 3*s* orbital for C was added to produce the band structure of graphene with the description of the electronic spectrum above the Fermi level close to the results of plane wave methods [40]. Moreover, for Ca, the 3*p* semicore state was included together with the valence states.

The charge density was projected onto a real-space grid with an equivalent kinetic energy cutoff of 200 Ry. Adsorption of the Ca atoms and hydrogen molecules was treated within the supercell geometry with lattice parameters $a_{SC} = b_{SC} = 4.92$ Å and $c_{SC} = 25$ Å for a (2×2) cell of graphene ($a_{SC} = b_{SC} = 9.85$ Å for a (4×4) cell). The distance between the graphene plane and its images (c_{SC}) is large enough to avoid any interactions. According to the Monkhorst–Pack scheme, [41] the Brillouin zone was sampled by $(31\times31\times1)$ and $(15\times15\times1)$ special mesh points in K space for (2×2) and (4×4) graphene cells, respectively. Full structural optimizations were carried out using the conjugate gradient (CG) algorithm until the maximum residual forces were less than 0.02 eV/Å and the total pressure of the system was smaller than 0.1 kbar per unit cell. The convergence criterion for energy was chosen as 10^{-5} eV between CG steps.

3. Results and discussions

We first consider pure graphene coated with Ca atoms, assuming that individual metal atoms are dispersed uniformly on the surface. As illustrated in Fig. 1, (2×2) and (4×4) cells of graphene (G(2×2) and G(4×4), respectively) with periodic boundary conditions (PBC) are considered to compare two different coverage densities of Ca. In G(2×2) (Fig. 1a), the average Ca–Ca distance is 4.96 Å, which is larger than that of bulk Ca (3.82 Å [25]), but still the Ca atoms have some interaction. However, a large distance of 9.85 Å in G(4×4) results in negligible interaction between Ca atoms.

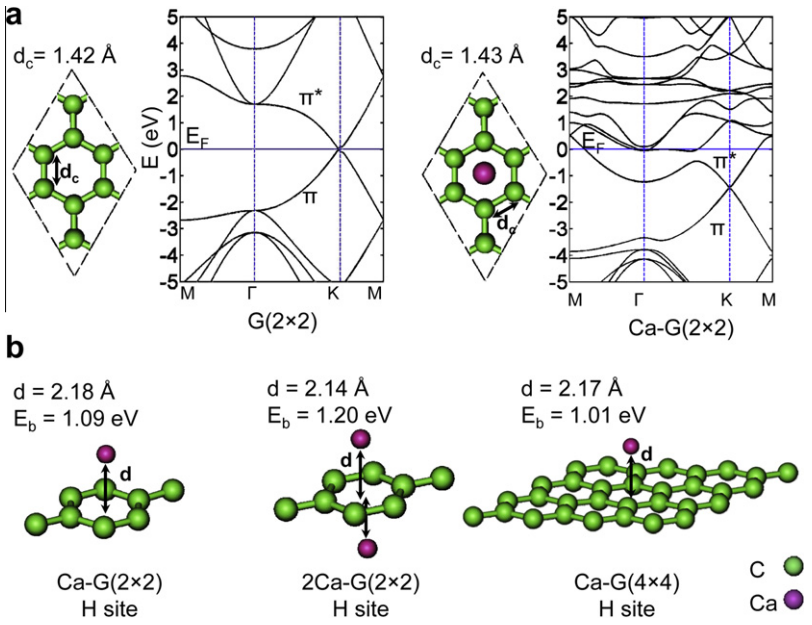

Fig. 1 – (a) The calculated energy band structures of G(2 × 2) and Ca-coated G(2 × 2) with PBC, assuming $E_F = 0$. Upon Ca adsorption, the π^* bands of graphene are occupied and distorted. (b) The optimized structure of a single Ca atom adsorbed on the H site of the (2 × 2) cell of graphene (Ca–G(2 × 2)), double-sided adsorption of Ca atoms on the H site of G(2 × 2) (2Ca–G(2 × 2)) and single-sided adsorption of Ca on a (4 × 4) cell of graphene (Ca–G(4 × 4)), and the calculated adsorption energies and bond lengths at the LDA level.

Our calculations show that the denser Ca coverage in G(2 × 2) is energetically more favorable and stable than G(4 × 4) (see binding energy (E_b) values in Fig. 1b), due to Ca's tendency to aggregate. We also investigated different sites of adsorption and found that the hollow site (H site) above the center of the hexagon is the most favorable site for both single- and double-sided adsorption. The E_b of a Ca atom adsorbed on a H site is 1.09 and 1.2 eV for single- and double-sided coverage, respectively. In the double-sided configuration, the increase in binding energy of the second Ca atom by 0.11 eV is due to the electric field induced by the first Ca atom. The results for binding energy values are consistent with earlier works on Ca-decorated carbon nanostructures (such as graphene (~1.14 eV and ~1.27 eV for single- and double-sided, respectively) [24], C_{60} fullerene and nanotubes) using plane-wave calculations. Yoon et al. [21] have found that Ca and Sr bind strongly on top of a hexagonal ring of a C_{60} fullerene with an energy of ~1.3 eV, which is roughly half of that of Ti. Yang et al. [25] have shown that the binding energies of Ca adsorbates with the coverage of 50% on (5, 0) and (4, 0) nanotubes are 1.62 and 1.94 eV, respectively. The higher binding energy observed for C_{60} and nanotubes in comparison to graphene corroborates the finding that Ca binding energy on the nanotubes with the same chirality decreases as the diameter of the tube increases (e.g. for the (7, 0) tube, E_b is 1.32 eV).

Similar to the binding mechanism of Ca on C_{60}, Ca donates its 4*s* electrons to graphene due to its relatively low ionization potential, and the donated electrons partially fill the π^* states. As the Ca atom is brought closer to the surface, an electric field, formed between Ca and graphene, leads to back-donation of some electrons to the empty 3*d* orbitals, resulting in a strong hybridization between the carbon π^* and calcium *d* states [11,12,21]. The resulting charge transfer (i.e. positive charge on the Ca atom), calculated by Mulliken population analysis, is ~0.36 and ~0.40 electrons for single- and double-sided coatings, respectively. The calculated band structures of G(2 × 2) and Ca-coated G(2 × 2) show that the empty π^* band in graphene accommodates the transferred charge and accordingly becomes distorted (Fig. 1a).

Fig. 2 demonstrates the optimized structures for the double-sided adsorption of hydrogen molecules on Ca-coated (2 × 2) cell of graphene with periodic boundary conditions (2Ca–G(2 × 2)). We observe that the dipole between Ca and graphene facilitates attraction of up to 4 H_2 molecules per Ca atom. When we add the fifth H_2 molecule, it cannot make a strong bond with the Ca atom (~0.17 eV/H_2 according to LDA). Table 1 summarizes the binding energies of the first four hydrogen molecules for both LDA and GGA methods, calculated by $E_{bn} = E_{(\text{host}+H_2)} - (E_{H_2} + E_{\text{host}})$. Here, E_{bn} represents the binding energy of the *n*th hydrogen molecule and E_{host} is the energy for the optimized structures including the $(n-1)$ hydrogen molecules adsorbed on 2Ca–G(2 × 2). The results show that hydrogen is adsorbed on Ca–G(2 × 2) with an average binding energy of ~0.43 eV and ~0.16 eV per hydrogen according to LDA and GGA, respectively. The overall trends in the GGA calculations are found to be similar to those obtained using LDA while the actual values of the adsorption energies are about half of the LDA values. These results are in good agreement with Ref. [21], where the calculated average H_2 binding energy on CaC_{60} is 0.2 eV/H_2 and 0.4 eV/H_2 according to GGA and LDA, respectively. The optimized hydrogen binding energy and bond lengths, shown in Table 1, do not change significantly for a higher number of H_2 molecules. This is in contrast to the case of early transition metals

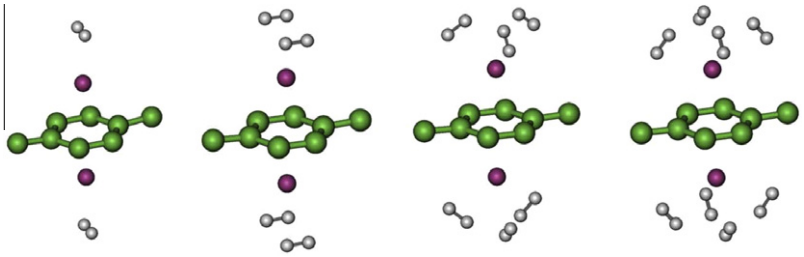

Fig. 2 – Optimized structures of double-sided Ca-decorated pure graphene (2Ca–G(2 × 2)) with one to four H_2 molecules, obtained by LDA calculations. In single and double H_2 adsorption on each Ca atom, the adsorbed molecules are parallel to graphene. The adsorbed H_2 molecules tend to tilt toward the Ca atom upon adding the third and fourth hydrogen molecules.

Table 1 – Average adsorption energies of hydrogen molecules on 2Ca–G(2 × 2) and the corresponding bond lengths for one to four adsorbed H_2 molecules per Ca atom. Both LDA (CA) and GGA (PBE) DFT-level calculation results are presented.

	E_b (eV/H_2)		d(H–Ca) (Å)		d(H–H) (Å)	
	LDA	GGA	LDA	GGA	LDA	GGA
2Ca-G(2 × 2)–H_2	0.254	0.075	2.29	2.42	0.81	0.83
G(2 × 2)2Ca–$(H_2)_2$	0.413	0.142	2.28	2.38	0.84	0.82
G(2 × 2)2Ca–$(H_2)_3$	0.609	0.270	2.21	2.27	0.87	0.84
G(2 × 2)2Ca–$(H_2)_4$	0.456	0.164	2.22	2.29	0.86	0.83

(i.e. Sc, Ti, and V), where the first hydrogen molecule is dissociated due to its strong interaction with the TM atoms [11,12]. Our calculated energies and relaxed structures are in good agreement with the earlier results obtained by plane-wave calculations [24]. Adsorption of four hydrogen molecules on each Ca atom in 2Ca–G(2 × 2) results in a hydrogen storage capacity of 8.32 wt.%.

In the above calculations, Ca atoms are assumed to be uniformly distributed on the graphene sheet. The calculated adsorption energy of Ca atoms with the average Ca–Ca distance of 4.96 Å on one side is smaller than the Ca cohesive energy. Thus, metal aggregation can take place on pure graphene. To have a stable and uniform decoration of individual Ca on graphene, the Ca–graphene adsorption energy must be more than the cohesive energy in the bulk Ca (~1.8 eV).

Our calculations show that substitutional boron doping can be used to prevent the clustering problem, as it increases the metal adsorption strength on graphene. As shown in Fig. 3, the adsorption energy of Ca is enhanced to 2.86, 2.98, and 3.82 eV for single, double, and triple B-doped configurations of (2 × 2) graphene (with single-sided Ca coating), respectively. These binding energies are much higher than the cohesive energy of Ca. The corresponding band structures (Fig. 3) show that in B-doped configurations the π and π^* bands are shifted above the Fermi level, as the empty p_z orbital of the boron acts as a strong charge accepting center. As a result, boron doping forms an electron-deficient structure and this deficiency increases as the number of B atoms increases. Charge transfer from Ca atom to graphene occurs more efficiently for these electron-deficient structures leading to stronger Ca–graphene binding.

To provide a more explicit analysis of metal stability in B-doped structures, we calculate the binding energy of a Ca dimer and two isolated Ca atoms on pure and B-doped (4 × 4) cell of graphene (Fig. 4). These calculations show that the dimerized Ca atom on pure graphene is energetically more favorable by ~0.4 eV as compared with the isolated case. In contrast, for the B-doped structure, the energy of the

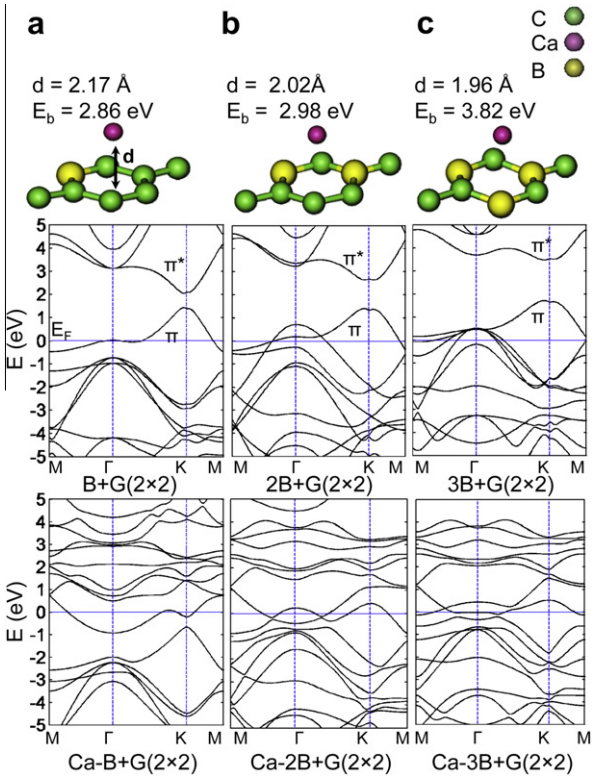

Fig. 3 – The optimized structures, binding energies, bond lengths and energy band diagrams of a single Ca atom adsorbed on the H site of (a) single (B + G(2 × 2)), (b) double (2B + G(2 × 2)), and (c) triple (3B + G(2 × 2)) configurations of a (2 × 2) graphene cell with PBC.

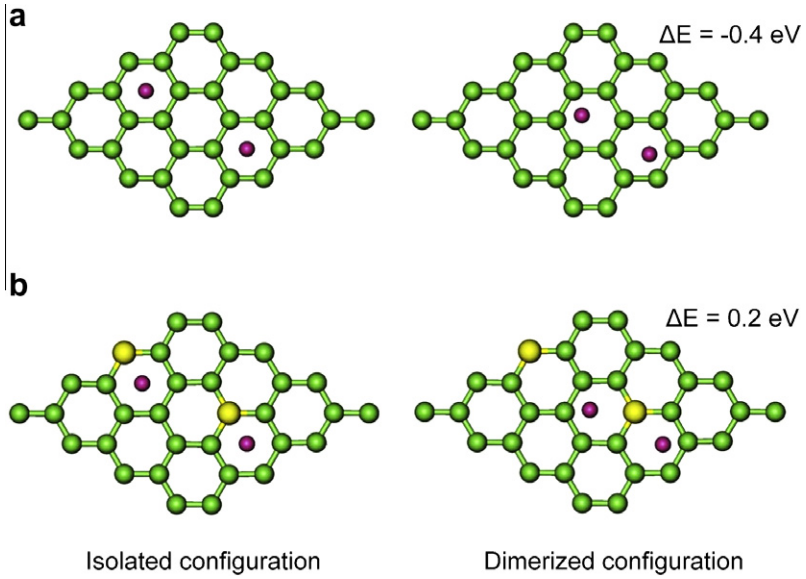

Fig. 4 – Optimized structures of dimerized and isolated Ca atoms adsorbed on (a) pure and (b) B-doped (4 × 4) cells of graphene. Our calculations show that in the B-doped structure the isolated configuration is energetically more favorable by ~0.2 eV (ΔE = 0.2 eV) while in the pure configuration the dimerized configuration is more stable by ~0.4 eV (ΔE = −0.4 eV).

isolated configuration is ~0.2 eV lower than that of the dimerized case. Therefore, Ca can be individually dispersed on a single B-doped graphene layer. In contrast to Ca, TM atoms (such as Sc, V and Ti) have been found to prefer the dimer form in single and pair B-doped graphene, while they form separated metal atoms in the triplet B-doped configuration [42]. It has been experimentally observed that B doping concentration in graphene can be up to 20 at.% [29,30]. Therefore, a triple B-doped configuration, with the doping concentration of ~38%, may not be a stable structure. Consequently, we can say that solving the clustering problem in Ca-decorated graphene could be more practical than that in TM-coated graphene.

Now, we investigate hydrogen adsorption on B-doped configurations using LDA calculations. For this study, we consider one-sided Ca coating and compare the binding energies of adsorbed H_2 molecules on different boron-doped configurations. Here, the maximum number of adsorbed H_2 per adsorbed Ca atom is still four for the (2 × 2) coverage similar to that of pure graphene. The average binding energies of the H_2 molecule on single, double, and triple configurations are ~0.42, ~0.39, and ~0.38 eV/H_2, respectively, which are close to the average E_b of H_2 molecules on pure graphene (~0.43 eV/H_2). However, for all configurations the binding energy of the first H_2 molecule decreases by ~0.1 eV in comparison to pure graphene.

The binding mechanism of H_2 on Ca decorated graphene has similarities to that of TM coated graphene. Two binding mechanisms contribute to the adsorption of H_2, namely, the polarization of the H_2 molecule under the electric field produced by the Ca–graphene dipole and the hybridization of the 3*d* orbitals of Ca with the σ orbitals of H_2 [23,24]. Fig. 5 illustrates the partial density of states (PDOS) for the H_2 σ and Ca 3*d* orbitals for two cases when one hydrogen molecule is adsorbed on a pure and a tri-B-doped graphene layer, respectively. The overlap between Ca 3*d* and H_2 σ just below the Fermi energy demonstrates the role of hybridization of the Ca 3*d* orbital in efficient adsorption of hydrogen molecules. As discussed by Ataca et al. [24], the effect of hybridization further increases when the second, third and fourth hydrogen molecules are adsorbed, due to broadening of the H_2 σ PDOS by virtue of H_2–H_2 interactions. However, for understanding the binding mechanism of H_2 on Ca decorated graphene, both hybridization and Coulomb interaction due to negative charging of H_2 must be considered. As seen in Fig. 5, while there is an increase in the overlap (between the Ca 3*d* and H_2 σ orbitals just below the Fermi energy) for the B-doped graphene in comparison to the pure one, the bond between the first H_2 and graphene is slightly stronger in the pure graphene. Mulliken charge populations calculations for each H atom, the Ca atom, and the B-doped graphene (or the pure graphene) are −0.048, 0.517, and −0.420 electrons (or −0.052, 0.396, and −0.295 electrons), respectively. The negative charge on each H atom is slightly lower for the B-doped graphene in comparison to the pure graphene, an indication of a weaker bond in the B-doped material. The charge on the Ca atom before hydrogen adsorption is 0.466 and 0.356 electrons for the B-doped and pure graphene, respectively. These charge calculations reveal that both the Ca atom and graphene transfer electron charge to H_2 molecule during adsorption. While for the B-doped graphene, calcium transfers more charge to H_2 (i.e. 0.517 − 0.466 = 0.051 electrons in comparison to 0.396 − 0.356 = 0.040 for the pure graphene), the B-doped graphene only back donates 0.046 electrons while the pure graphene donates 0.064 electrons. The smaller back donation of the B-doped graphene can be attributed to its stronger electron accepting property due to boron doping and is the underlying mechanism for its weaker binding with the hydrogen molecule.

The above calculations were performed using DFT, and the accuracy of the relatively weak binding energies obtained with this method is questionable. As Table 1 shows, binding energies calculated with LDA are more than those of GGA

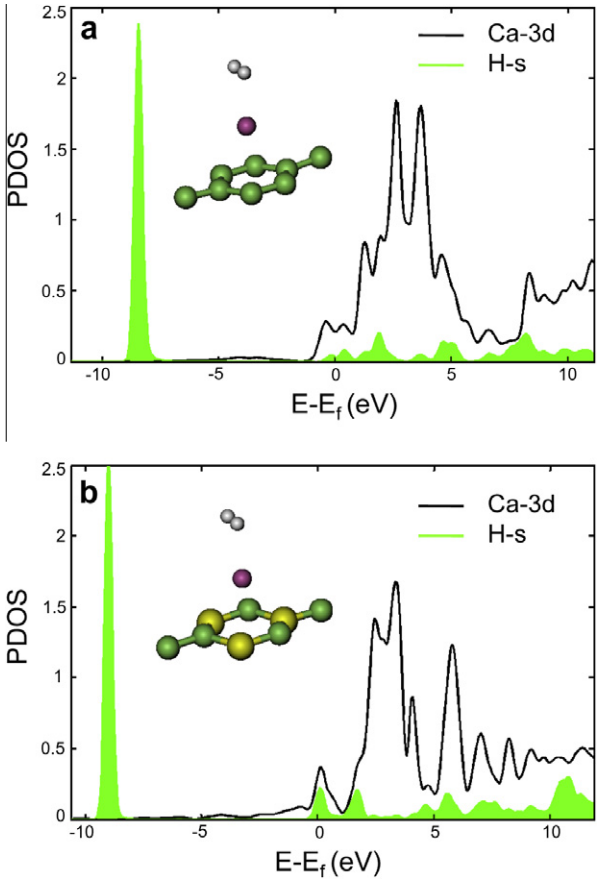

Fig. 5 – Partial density of states (PDOS) of the Ca 3*d* orbitals and H_2 σ (H-s) orbitals involved in the adsorption of hydrogen on a Ca-decorated (a) pure graphene and (b) triple B-doped configuration. The Fermi energy E_F is set to zero.

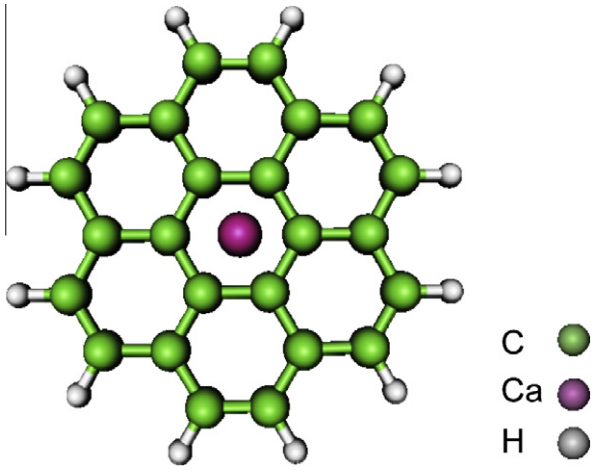

Fig. 6 – Structure of Ca attached to a pure coronene molecule. This molecular model has previously been shown to provide an adequate representation of graphene for the purpose of binding energy calculations [43].

results. To evaluate our DFT calculations, we performed MP2 simulations. MP2 is expected to provide a good description of dispersive interactions, which is missing in DFT calculations.

Table 2 – Comparison of binding energies (in eV) and bond lengths (in Å) obtained by LDA (SVWN5), GGA (PBE), and MP2 calculations on the molecular model of Coronene.

	d(Ca–C)	*d*(H–Ca)	*d*(H–H)	E_b(Ca–C)	E_b(H–Ca)
SVWN5	3.30	4.56	0.77	0.233	0.007
PBE	4.08	6.81	0.75	0.007	0.002
MP2	3.60	5.30	0.73	0.382	0.005

The comparison was carried out with the GAUSSIAN 03 package [44] using the molecular model of coronene (six benzene rings passivated with hydrogen) as a model for a graphene fragment (PBCs are not available for MP2 in GAUSSIAN) (Fig. 6). This model has previously been shown to provide an adequate representation of graphene for the purpose of binding energy calculations [43]. The structural optimizations and binding energy calculations were performed using double-zeta polarized 6-31G(d,p) and triple-zeta polarized 6-311G(d,p) basis sets, respectively. In our DFT calculations in GAUSSIAN, GGA is described by the PBE functional. Also, LDA is described by the Slater exchange plus Vosko–Wilk–Nusair correlation (SVWN5) [45], which fits the Ceperely–Alder solution to the uniform electron gas [46]. The results are summarized in Table 2. It can be seen that overall, LDA results are a better match to those of MP2 for both energies and structures. This gives us further confidence about the validity of the trends predicted by our LDA simulations.

4. Conclusions

In conclusion, we have studied the metal dispersion and hydrogen binding properties on Ca-coated B-doped graphene. It is found that a stable and uniform decoration of individual Ca atoms on graphene can be obtained upon substitutional boron doping. Our calculations show that individual calcium atoms are stable on a single B-doped (2×2) cell of graphene (i.e. with a concentration of 12 at.% boron doping). The double-sided Ca-decorated single B-doped graphene (2Ca−B + G(2×2)) can reach a gravimetric capacity of 8.38 wt.%. These results are critical for guiding experimental works on the development and synthesis of carbon-based nanomaterials (such as graphene) for hydrogen storage systems that can operate at room temperature and ambient pressure.

Acknowledgements

We gratefully acknowledge the financial support of the Natural Sciences and Engineering Research Council (NSERC) of Canada for this project. This research has been enabled by the use of computing resources provided by WestGrid and Compute/Calcul Canada.

REFERENCES

[1] Schlapbach L, Züttel A. Hydrogen-storage materials for mobile applications. Nature 2001;414:353–8.

[2] Bhatia SK, Myers AL. Optimum conditions for adsorptive storage. Langmuir 2006;22(4):1688–700.
[3] Lochan RC, Head-Gordon M. Computational studies of molecular hydrogen binding affinities: the role of dispersion forces, electrostatics, and orbital interactions. Phys Chem Chem Phys 2006;8(12):1357–70.
[4] Dillon AC, Jones KM, Bekkedahl TA, Kiang CH, Bethune DS, Heben MJ. Storage of hydrogen in single-walled carbon nanotubes. Nature 1997;386(6623):377–9.
[5] Chambers A, Park C, Baker RTK, Rodriguez NM. Hydrogen storage in graphite nanofibers. J Phys Chem B 1998;102(22):4253–6.
[6] Liu C, Fan YY, Liu M, Cong HT, Cheng HM, Dresselhaus MS. Hydrogen storage in single-walled carbon nanotubes at room temperature. Science 1999;286(5442):1127–9.
[7] Ritschel M, Uhlemann M, Gutfleisch O, Leonhardt A, Graff A, Täschner C, et al. Hydrogen storage in different carbon nanostructures. Appl Phys Lett 2002;80(6):2985–7.
[8] Hirscher M, Becher M, Haluska M, Quintel A, Skakalova V, Choi YM, et al. Hydrogen storage in carbon nanostructures. J Alloys Compd 2002;330:654–8.
[9] Panella B, Hirscher M, Roth S. Hydrogen adsorption in different carbon nanostructures. Carbon 2005;43(10): 2209–14.
[10] Zhang Y, Franklin NW, Chen RJ, Dai HJ. Metal coating on suspended carbon nanotubes and its implication to metal–tube interaction. Chem Phys Lett 2000;331(1):35–41.
[11] Yildirim T, Ciraci S. Titanium-decorated carbon nanotubes as a potential high-capacity hydrogen storage medium. Phys Rev Lett 2005;94(17):175501.
[12] Zhao YF, Kim YH, Dillon AC, Heben MJ, Zhang SB. Hydrogen storage in novel organometallic buckyballs. Phys Rev Lett 2005;94(15):155504.
[13] Durgun E, Ciraci S, Yildirim T. Functionalization of carbon-based nanostructures with light transition-metal atoms for hydrogen storage. Phys Rev B 2008;77(8):085405.
[14] Michael D, Mingos P. A historical perspective on Dewar's landmark contribution to organometallic chemistry. J Organomet Chem 2001;635(1–2):1–8.
[15] Kubas GJ. Molecular hydrogen complexes: coordination of a σ bond to transition metals. Acc Chem Res 1988;21:120–8.
[16] Sun Q, Wang Q, Jena P, Kawazoe Y. Clustering of Ti on a C_{60} surface and its effect on hydrogen storage. J Am Chem Soc 2005;127(42):14582–3.
[17] Durgun E, Ciraci S, Zhou W, Yildirim T. Transition-metal-ethylene complexes as high-capacity hydrogen-storage media. Phys Rev Lett 2006;97(22):226102.
[18] Chen P, Wu X, Lin J, Tan KL. High H_2 uptake by alkali-doped carbon nanotubes under ambient pressure and moderate temperatures. Science 1999;285(5424):91–3.
[19] Yang RT. Hydrogen storage by alkali-doped carbon nanotubes revisited. Carbon 2000;38(4):623–41.
[20] Dag S, Ozturk Y, Ciraci S, Yildirim T. Adsorption and dissociation of hydrogen molecules on bare and functionalized carbon nanotubes. Phys Rev B 2005;72(15):155404.
[21] Yoon M, Yang S, Hicke C, Wang E, Geohegan D, Zhang Z. Calcium as the superior coating metal in functionalization of carbon fullerenes for high-capacity hydrogen storage. Phys Rev Lett 2008;100(20):206806.
[22] Li M, Li YF, Zhou Z, Shen PW, Chen ZF. Ca-coated boron fullerenes and nanotubes as superior hydrogen storage materials. Nano Lett 2009;9(5):1944–8.
[23] Lee H, Ihm J, Cohen ML, Louie SG. Calcium-decorated carbon nanotubes for high-capacity hydrogen storage: first-principles calculations. Phys Rev B 2009;80(11):115412.
[24] Ataca C, Aktürk E, Ciraci S. Hydrogen storage of calcium atoms adsorbed on graphene: first-principles plane wave calculations. Phys Rev B 2009;79(4):041406.
[25] Yang XB, Zhang RQ, Ni J. Stable calcium adsorbates on carbon nanostructures: applications for high-capacity hydrogen storage. Phys Rev B 2009;79(7):075431.
[26] Sun YY, Lee K, Kim Y, Zhang SB. Ab initio design of Ca-decorated organic frameworks for high capacity molecular hydrogen storage with enhanced binding. Appl Phys Lett 2009;95(3):033109.
[27] Novoselov KS, Geim AK, Morozov SV, Jiang D, Zhang Y, Dubonos SV, et al. Electric field effect in atomically thin carbon films. Science 2004;306(5696):666–9.
[28] Züttel A, Sudan P, Mauron P, Kiyobayashi T, Emmenegger C, Schlapbach L. Hydrogen storage in carbon nanostructures. Int J Hydrogen Energy 2002;27:203–12.
[29] Way BM, Dahn JR, Tiedje T, Myrtle K, Kasrai M. Preparation and characterization of B_xC_{1-x} thin films with the graphite structure. Phys Rev B 1992;46(3):1697–702.
[30] Shirasaki T, Derré A, Ménétrier M, Tressaud A, Flandrois S. Synthesis and characterization of boron-substituted carbons. Carbon 2000;38(10):1461–7.
[31] Soler JM, Artacho E, Gale JD, García A, Junquera J, Ordejón P, et al. The SIESTA method for ab initio order-N materials simulation. J Phys-Condens Matter 2002;14(11):2745–79.
[32] Kleinman L, Bylander DM. Efficacious form for model pseudopotentials. Phys Rev Lett 1982;48(20):1425–8.
[33] Troullier N, Martins JL. Efficient pseudopotentials for plane-wave calculations. Phys Rev B 1991;43(3):1993–2006.
[34] Perdew JP, Zunger A. Self-interaction correction to density-functional approximations for many-electron systems. Phys Rev B 1981;23(10):5048–79.
[35] Perdew JP, Burke K, Ernzerhof M. Generalized gradient approximation made simple. Phys Rev Lett 1996;77(18):3865–8.
[36] Okamoto Y, Miyamoto Y. Ab initio investigation of physisorption of molecular hydrogen on planar and curved graphenes. J Phys Chem B 2001;105(17):3470–4.
[37] Kim YH, Zhao YF, Williamson A, Heben MJ, Zhang SB. Nondissociative adsorption of H_2 molecules in light-element-doped fullerenes. Phys Rev Lett 2006;96(1):016102.
[38] Moller CHR, Plesset MS. Note on an approximation treatment for many-electron systems. Phys Rev 1934;46(7):618–22.
[39] Louie SG, Froyen S, Cohen ML. Nonlinear ionic pseudopotentials in spin–density–functional calculations. Phys Rev B 1982;26(4):1738–42.
[40] Machón M, Reich S, Thomsen C, Sánchez-Portal D, Ordejón P. Ab initio calculations of the optical properties of 4-Å-diameter single-walled nanotubes. Phys Rev B 2002;66(15):155410.
[41] Monkhorst HJ, Pack JD. Special points for Brillouin-zone integrations. Phys Rev B 1976;13(12):5188–91.
[42] Kim G, Jhi SH, Park N, Louie S, Cohen ML. Optimization of metal dispersion in doped graphitic materials for hydrogen storage. Phys Rev B 2008;78(8):085408.
[43] Heine T, Zhechkov L, Seifert G. Hydrogen storage by physisorption on nanostructured graphite platelets. Phys Chem Chem Phys 2004;6(5):980–4.
[44] Frisch MJ, Trucks GW, Schlegel HB, Scuseria GE, Robb MA, Cheeseman JR, et al. GAUSSIAN 03, Revision C.02. 2004. Gaussian, Inc., Wallingford, CT.
[45] Vosko SH, Wilk L, Nusair M. Accurate spin–dependent electron liquid correlation energies for local spin density calculations: a critical analysis. Can J Phys 1980;58(8):1200–11.
[46] Ceperley DM, Alder BJ. Ground state of the electron–gas by a stochastic method. Phys Rev Lett 1980;45(7):566–9.